

The Exploration of Metabolic Biomarkers blood Lipidomics and Proteomics for Diagnosing Alzheimer's Disease.

J Tingyu Zhao¹, Ting Wang², Zihui Sun^{1,3}, Lixing Liu¹, Haiyan Wu¹, Li Zhang¹, Li Ma¹, Xueling Sun¹, Yuyao Yuan⁴, Fan Mei⁴, Yuxin Yin^{4*}, and Shouzi Zhang^{1†}

Received date: 30-Apr-2026, Manuscript No. NPY-26-189203; **Editor assigned date:** 02-May-2026, Manuscript No. NPY-26-189203 (PQ); **Reviewed date:** 18-May-2026, QC No. NPY-26-189203; **Revised date:** 25-May-2026, Manuscript No. NPY-26-189203 (R); **Published date:** 01-Jun-2026, DOI: 10.37532/1758-2008.2026.17(1).790

ABSTRACT

Introduction: Alzheimer's Disease (AD) is the most common neurodegenerative disorder; however, its underlying mechanisms remain incompletely understood, posing challenges for early diagnosis. This study aimed to explore potential metabolic biomarkers for AD in blood.

Methods: We recruited 82 participants, including 47 AD patients (age: 80.2 ± 0.9 years) and 35 healthy controls (age: 77.6 ± 1.7 years). Blood samples were collected and analyzed using liquid chromatography-tandem mass spectrometry (LC-MS/MS) and high-performance liquid chromatography coupled with Q-Exactive HPLC-MS. Data processing was performed using MS-DIAL, Skyline, and MaxQuant software. Metabolic pathway analysis was conducted with MetaboAnalyst, and enrichment analysis of differential metabolites was based on the KEGG database.

Results: Significant alterations were observed in amino acid metabolic pathways, including lysine degradation, pyruvate metabolism, glycine, serine and threonine metabolism, linolenic acid metabolism, and arginine and proline metabolism. Lipidomics analysis revealed seven lipids that were significantly elevated in the AD group: Cer 40:9;O3, DG 25:0, DG 46:7, NAE 16:1, PC 20:1/22:5, PC O-35:5, and TG 45:7. Notably, Receiver Operating Characteristic (ROC) curve analysis showed that the Area Under the Curve (AUC) values for these seven lipids all exceeded 0.8.

Discussion: This comprehensive multi-omics approach effectively identified dysregulated plasma molecules in AD patients, suggesting that specific blood lipids may serve as potential biomarkers for AD diagnosis.

Keywords: Alzheimer's disease; Amino acid; Lipidomics; Metabolic biomarker; Proteomics

Abbreviations: AA: Arachidonic Acid; Ach: Acetylcholine; Ac-PUT: N1-Acetyl-Putrescine; Ac-

¹Department of Psychiatry, Beijing Geriatric Hospital, Beijing 100069, China

²Department of Psychiatry, Children's Medical Center of Peking University First Hospital, Beijing, 102627, China

³Zhejiang Provincial Clinical Research Center for Mental Disorders, School of Mental Health, Wenzhou Medical University, Wenzhou, Zhejiang, 325035, P.R. China

⁴Department of Psychiatry and Neuroscience, Institute of Systems Biomedicine, School of Basic Medical Sciences, Peking University Health Science Center, Beijing, 100191, China

***Author for Correspondence:** Shouzi Zhang, Department of Psychiatry, Beijing Geriatric Hospital, Beijing 100069, China; email: lanczsz@126.com; Yuxin Yin, Department of Psychiatry and Neuroscience, Institute of Systems Biomedicine, School of Basic Medical Sciences, Peking University Health Science Center, Beijing, 100191, China; email: yinyuxin@bjmu.edu.cn

SPM: N1-Acetylspermine; AD: Alzheimer's Disease; CE-MS: Capillary Electrophoresis-Mass Spectrometry; Cers: Ceramides; CI: Chemical Ionization; CL: Cardiolipin; CNS: Central Nervous System; DG: Diacylglycerol; dAMP: Deoxyadenosine Monophosphate; DCA: Deoxycholic Acid; DHA: Docosahexaenoic Acid; DI-MS: Direct Infusion Mass Spectrometry; ESI: Electrospray Ionization; GCMS: Gas Chromatography-Mass Spectrometry; GDCA: Glycodeoxycholic Acid; GLCA: Glycolithocholic Acid; GlcNAc: N-Acetyl-D-glucosamine; GPC: Glycerophosphocholine; GPs: Glycerophospholipids; HCD: High-Energy Collision Dissociation; HILIC: Hydrophilic Interaction Liquid Chromatography; HPLC-MS: High-Performance LC-MS; KEGG: Kyoto Encyclopedia of Genes and Genomes; LC-MS: Liquid Chromatography-Mass Spectrometry; LPAs: Lysophosphatidic Acids; LysoPC or LPC: Lysophosphatidylcholine; LysoPE or LPE: Lysophosphatidylethanolamine; MG: Monoacylglycerol; MCI: Mild Cognitive Impairment; MUFAs: Monounsaturated Fatty Acids; NAD: Nicotinamide Adenine Dinucleotide; NMR: Nuclear Magnetic Resonance; PA: Phosphatidic Acid; PC: Phosphatidylcholine; PCae: Acyl-Alkyl Phosphatidylcholines; PE: Phosphatidylethanolamine; PG: Phosphatidylglycerol; PI: Phosphatidylinositol; PLA2: Phospholipase A₂; PLS: Phospholipids; PS: Phosphatidylserine; PS1 and PS2: Presenilin 1 and 2; pTau: Hyperphosphorylated Tau; RP: Reversedphase; S1P: Sphingosine 1-Phosphates; SAH: S-Adenosyl-Homocysteine; SDMA: Symmetric Dimethylarginine; SFAs: Saturated Fatty Acids; SM: Sphingomyelin; TG: Triacylglycerol; TCA cycle: Citrate Cycle; TLCA: Taurolithocholic Acid; TQ-MS: Triple Quadrupole-Mass Spectrometry; tTau: Total Tau; UHPLC or UPLC: Ultra-HPLC; UPLC-MS: Ultra-performance Liquid Chromatography-Mass Spectrometry; WGCN: Weighted Correlation Network Analysis

Introduction

Early screening and diagnosis have become increasingly important with the rising incidence of Alzheimer's Disease (AD). Amyloid-beta (A β) and tau protein are two core biomarkers of AD [1]. Currently, cerebrospinal fluid (CSF) biomarkers and amyloid Positron Emission Tomography (PET) imaging are not widely applied in clinical practice due to their invasiveness, limited accessibility, and high costs. Compared with CSF or PET examinations, plasma biomarkers are less invasive, more cost-effective, and easier to implement. However, accurately quantifying A β in blood remains challenging due to its low concentration [2]. However, with the continuous improvement of detection technology, plasma biomarker detection has become the mainstream direction for AD diagnosis in the future. Food and Drug Administration (FDA) approved the first *in vitro* diagnostic device, the Lumipulse G pTau217/ β -Amyloid 1-42 Plasma Ratio, for clinical use to aid in the diagnosis of AD [3]. Metabolomics, which studies the complete set of metabolites within cells at a specific time point, reflects the cellular microenvironment [4,5]. With the rapid advancement of Liquid Chromatography-Mass Spectrometry (LC-

MS)-based omics technologies [5], it is now feasible to reliably analyze hundreds to thousands of metabolites from biological samples, providing valuable insights for biomarker discovery as well as pathological and biological research [6,7]. Consistent with this, several metabolites have been found to be dysregulated in the blood of AD patients [8], suggesting their potential utility as diagnostic markers for AD [9]. The combination of plasma metabolomic biomarkers with plasma A β biomarkers may enable more accurate early diagnosis of AD. We plan to conduct a plasma metabolomics study comparing Alzheimer's disease patients with elderly cognitively normal controls, with the aim of discovering potential biomarkers for early diagnosis and treatment of AD.

Methods and Materials

■ Participants

Data were collected between January and May 2024 from a geriatric hospital and a nursing community. The cohort included cognitively normal controls (n=35; mean age=77.57 \pm 1.65 years) and patients with clinically diagnosed AD (n=47; mean age=80.15 \pm 0.94 years). AD diagnosis was made based

on recommendations from the National Institute on Aging-Alzheimer's Association workgroups on diagnostic guidelines for Alzheimer's disease [10].

■ Ethical Statement

This study was approved by the Clinical Ethics Committee of Beijing Geriatric Hospital (Ethical Approval Number: BJLLYY-2024-009), in compliance with the principles of the Helsinki Declaration. Samples were collected only from patients who agreed to undergo this examination for laboratory research. The informed consent of blood donors was obtained, and all methods were conducted according to relevant guidelines and regulations.

■ Metabolomics Sample Processing

After fasting overnight, collect 4 mL of venous blood from the forearm circulation and transfer it to an EDTA-K2 vacuum tube. Centrifuge at $3000 \times g$ for 20 minutes to separate the plasma, then store at -80°C until analysis. Use liquid-liquid extraction to extract metabolites and lipids from the plasma sample as follows: extract 100 μL of plasma with four times its volume of cold chloroform:methanol (2:1). Vortex the mixture and centrifuge at $13,000 \times g$ for 15 minutes. Collect the upper aqueous phase (hydrophilic metabolites) and the lower organic phase (hydrophobic metabolites), and vacuum evaporate under room temperature. Store the evaporated samples at -80°C until LC-MS/MS analysis.

■ HPLC and Q-Exactive HF MS for Metabolomics

Metabolomics and lipidomics were performed on the Ultimate 3000 ultra-high-performance liquid chromatography system and Q-Exactive HF MS (Thermo Scientific). The aqueous phase (metabolites) was separated using a Xbridge amide column ($100 \times 2.1 \text{ mm i.d.}, 3.5 \mu\text{m}$; Waters), under 30°C . Compounds were separated at 30°C . Mobile phase A consists of 5 mM ammonium acetate aqueous solution, and mobile phase B is acetonitrile. Flow rate is 0.4 mL/min, with a linear gradient as follows: 0 minutes, 95% B; 3 minutes, 90% B; 13 minutes, 50% B; 14 minutes, 50% B; 15 minutes, 95% B; 17 minutes, 95% B. Samples were suspended in a 100 μL acetonitrile: water (1:1, v/v) solution, with an injection volume of 10 μL . Injection volume is 10 μL . Chromatographic

separation of lipids was performed using an inverse-phase X-select CSH C18 column ($2.1 \text{ mm} \times 100 \text{ mm}, 2.5 \mu\text{m}$, Waters Corporation) at a separation temperature of 40°C . A binary solvent system was used (containing 10 mM ammonium acetate and 0.1% formic acid) for the gradient. Elution: (A) ACN/water (3:2, V/V), (B) IPA/ACN (9:1, V/V). The gradient procedure is as follows: 0 minutes-40% B; 2 minutes-43% B; 12 minutes-60% B; 12.1-75% B; 18 minutes-99% B; 19 minutes-se the flow rate to 0.4 mL/min. The sample is suspended in a 100 μL chloroform: methanol (1:1, v/v) solution and then diluted three times with isopropanol. It is further diluted three times with an isopropanol:acetonitrile:H₂O (2:1:1, v/v/v) solution. The injection volume is 10 microliters.

■ Mass Spectrometry for Metabolomics

Mass spectrometry techniques used for metabolomics are based on Data-Dependent Acquisition (DDA) and Parallel Reaction Monitoring (PRM) on Q-Exactive HF MS (Thermo Scientific). For DDA-MS, acquisition is performed separately in positive and negative ion mode. Each acquisition cycle includes one (MS1 scan) with a resolution of 60,000, covering the mass range of hydrophilic metabolites from 60 to 900 m/z, followed by 10 MS/MS scans in HCD mode. Ten MS/MS scans are performed at 30,000 resolutions. For PRM-MS, the m/z values for 14 target lipids (13 target lipids and 1 internal standard) are set in the inclusion list, with each acquisition cycle including one full MS1 scan at a resolution of 60,000 (from 200 m/z to 1200 m/z) and 14 MS2 scans targeting the specified lipid at 30,000 resolutions.

For DDA-MS and PRM-MS, the Automatic Gain Control (AGC) target values are both set to 5e6 (maximum injection time 30 ms) and 2e5 (maximum injection time 100 ms). MS1 and MS/MS scans. Ion source parameters: spray voltage of 3.3 kV in positive ion mode, and 3.0 kV in negative ion mode. Spray voltage of 3.3 kV in positive ion mode, and 3.0 kV in negative ion mode; ion source sheath gas 40; auxiliary gas 10; capillary temperature 320°C ; probe heater temperature 300°C ; S-lens RF level 55. Samples (a total of 100) are analyzed in random order. Quality Control (QC) samples: all research samples are mixed equally and analyzed every 10 samples throughout the

chromatographic analysis process. Throughout the liquid chromatography-mass spectrometry analysis, one analysis is performed every 10 samples.

■ DDA-MS Data Analysis for Metabolomics

According to the user guide, process the raw data collected from DDA-MS on MS-DIAL software. In short, use the Reifycs ABF converter (<http://www.reifycs.com/AbfConverter/index.html>) to convert the raw MS data from the supplier's file format (.wiff) to the universal file format (.abf) in Reifycs Inc.. After conversion, use MS-DIAL software for feature detection, spectral deconvolution, metabolite identification, and peak alignment between samples. Obtain the MS/MS spectra from the Mass Bank database provided by MS-DIAL software and perform MS/MS based metabolite identification in MS-DIAL using the obtained MS/MS spectra. The MS and MS/MS information containing metabolites are included in MS-DIAL. Perform lipid identification based on MS spectra by searching the obtained MS/MS spectra in MS-DIAL. The internal computer of the software simulates the MS spectrum database for MS/MS spectra (version number: LipidDBs-VS 23-Fiehn0, which includes MS and MS/MS information for common lipid types. The tolerance settings for MS and MS/MS searches are set to 0.01 Da and 0.05 Da, and other parameters used in MS-DIAL are set to the default values.

■ PRM MS Data Analysis

According to the plan (<https://www.example.com/project/home/software/Skyline/start.view>), process the raw data on Skyline software. Import the original MS data file into the software for peak extraction. Pre-select an adsorbent-product ion pair (transition) for each target lipid, and calculate the peak area corresponding to each transition using the software. Finally, export the results containing lipid identification and quantification in tabular form for further statistical analysis.

■ Proteomics Sample Preparation

A total of 47 AD patients and 35 healthy controls were used for proteomics studies. According to the manufacturer's recommendations, plasma (4 μ L crude plasma) was subjected to Multiple Affinity Removal System (MARS) Human-14

column (Agilent) to remove high-abundance proteins. The fractions were collected (low-abundance proteins), then digested according to the manufacturer's Filter Assisted Sample Preparation (FASP) protocol. Proteins were digested overnight in 50 mM NH_4HCO_3 buffer at a protein-to-enzyme ratio of 50:1 with trypsin at 37°C, and the released peptides were collected by centrifugation and evaporated under vacuum.

■ LC-MS Analysis for Proteomics

The sample (1 μ g) was analyzed on a self-made C18 column (75 $\mu\text{m} \times 500\text{mm}$, 3 μm) of the U3000 ultra-high-performance liquid chromatography system is connected to the Q Exactive HF mass spectrometer (Thermo Scientific). Peptides were separated by linear gradient elution from 5% to 35% ACN containing 0.1% formic acid over 60 minutes at a flow rate of 300 nL/min, and then increased linearly to 80% ACN within 1 minute. Increased linearly to 80% ACN within 1 minute and maintained for 3 minutes. The column was rebalanced in 5% acetonitrile for 5 minutes. Rebalanced for 5 minutes. The operating voltage of the chromatographic source is 2.1 kV. The DDA scheme includes full MS scans with a resolution of 60,000 FWHM (at m/z 200), set to AGC 5E6 (maximum injection time 20 ms). Set to AGC 5E6 (maximum injection time 20 milliseconds), followed by 20 MS/MS scans with a resolution of 15,000 FWHM, set to AGC 5E6 (maximum injection time 20 milliseconds). Then perform 20 MS/MS scans with a resolution of 15,000 FWHM, AGC set to 2E5 (maximum injection time of 100 milliseconds).

Select the 20 most intense precursors, with a separation width of m/z 2 for High-energy Collision Dissociation (HCD) fragmentation, followed by 27 HCD fragmentation. Set dynamic exclusion to 30 seconds. Obtain the profile type. (For details, see supplementary information). Data analysis is performed using MaxQuant software version 1.6.2.0. (<http://www.maxquant.org/>) for data analysis. To identify proteins, MS/MS data is submitted to the uniProt human proteome database (3.43 version, 72,340 sequences). The Andromeda search engine is used to submit to the uniProt human proteome database (3.43 version, 72,340 sequences), with the following settings: trypsin digestion; fixed modifications: cysteine methylation; variable modifications: methionine oxidation; maximum modification:

cysteine methylation. Variable modification for methionine oxidation; up to two missed cleavages; false discovery rate calculated from the search bait database. Other parameters are set to default values. Unlabeled Quantification (LFQ) was also performed in MaxQuant. The minimum ratio count for LFQ is set to 2, and the run-to-run matching option is set to 1 minute. Other parameters are set to their default values. Other parameters are set to their default values.

Statistical Analysis

Statistical analysis was performed using SPSS 26.0 software. All results were analyzed using ANOVA or Student's t-test, with mean ± standard error notation. A p<0.05 was considered statistically significant. UPLC-Q-TOF/MS technology was used to collect spectral information, and peak identification, peak matching, Retention Time (RT), and Mass (M/Z) data from XCMS and VGDB were compared. Three-dimensional data information was imported into R software.

Principal Component Analysis (PCA) and Partial Least Squares Discriminant Analysis (PCA-da) were used to obtain clustering information and important variables. PLS-DA model was employed to calculate VIP values for each variable in the sample. Metabolites with VIP>1.05 were selected as differentially expressed metabolites at various time points across groups.

Data was normalized and transformed logarithmically, and t-tests were used to calculate P values. When there was no biological replication, one-fold changes were calculated.

Metabolites with log2-fold change ≥ 1 and P ≤ 0:05 were selected as the final differentially expressed metabolites. Qualitative analysis of primary and secondary spectra data from mass spectrometry was conducted based on Very Genome Database (VGDB), and substance analysis was performed by referencing other public mass spectrometry databases such as MassBank, METLIN, HMDB, and MONA. Finally, the metabolic pathway analysis was performed using MetaboAnalyst 5.0 (<https://www.metaboanalyst.ca/>).

Results

Overview of Research Workflow

Blood plasma samples were collected from 47 AD patients and 35 control plasma samples from the general population. The age, gender, and MMSE scores of AD patients compared with the normal control group are shown in Table S1. Non-targeted metabolomics, lipidomics, and proteomics studies based on LC-MS were conducted to identify biomolecules that may be dysregulated in AD patient plasma. Statistical analysis and data mining revealed abnormal expression of certain metabolites, lipids, and proteins in AD patients. Bioinformatics analysis elucidated the abnormal expression of these metabolites, and targeted quantitative analysis using LC-MS (PRM) was employed to validate some of the omics results. Finally, ROC curves for dysregulated molecules were calculated, along with their correlation with clinical factors in AD, to evaluate their potential use as biomarkers for AD diagnosis or prognosis (Figure 1).

Table S1 Clinical information of the subjects in the study.

	AD (n=47)	NC (n=35)	P-value
Age, mean ± SE	83.15 ± 0.94	77.57 ± 1.65	0.0632a
Gender (m/f)	25/22	19/16	0.9217b
Duration of disease (year), mean ± SE		/	
Cognitive impairment (mild/moderate/severe)	01-08-1938	/	
MMSE, Mean ± SE	3.213 ± 0.6915	27.57 ± 0.2020	<0.000a

Note: AD: Alzheimer's Disease; NC: Normal Control; A: Student t-test was used to analyze the statistical significance of age and MMSE between AD and NC. Notably, there were significant differences in MMSE between AD and NC groups. b: Differences in gender composition between groups were calculated using the χ^2 test.

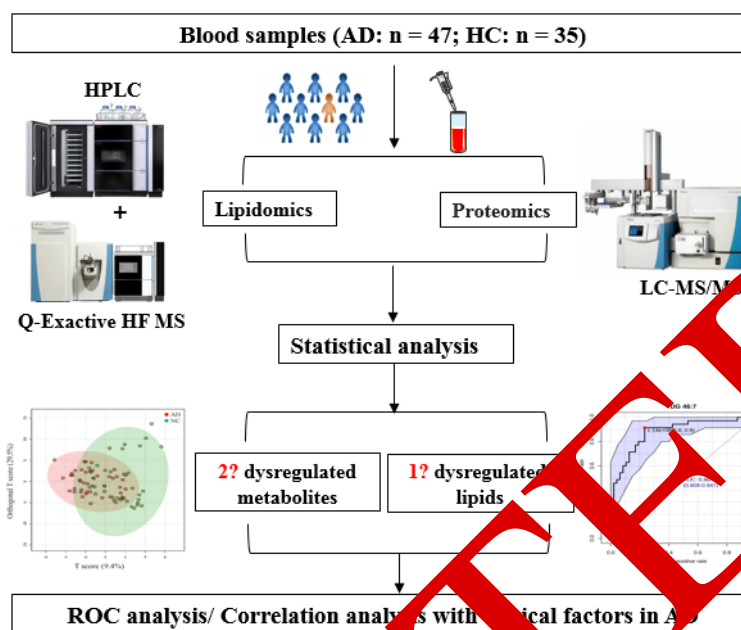


Figure 1. Flowchart of the study workflow. Eighty participants were included in the study, of which 47 were AD patients, 35 healthy volunteers were included as a control group. In the discovery stage, untargeted lipidomics and proteomics were performed to investigate dysregulated molecules in the blood. Pathway enrichment, correlation analysis and ROC analysis were performed to further gain insights from the omics data.

■ **Metabolomics Analysis and Dysregulated Metabolites in AD**

After processing the raw MS data, Principal Component Analysis (PCA) was used to obtain an overview of the metabolites expression profiles of all samples in both positive ion (Figure 2A) and negative ion (Figure 2B) modes. On the PCA score plot, the AD group and the control group show a clear separation trend. Further statistical analysis revealed a total of 31 dysregulated metabolites (23 in positive ion mode (Figure 2C); 8 in negative ion mode (Figure 2D) (FC > 2 and t-test p-value < 0.05). Additionally, MetaboAnalyst was used to analyze metabolic pathways with significant differences between the AD group and the HC group.

■ **Lipidomics Analysis and Lipid Dysregulation in AD**

For the data processing procedures for metabolomics features, PCA is used to summarize the expression patterns of lipids in all samples. Similarly, the results of metabolomics features, both the AD group and the control group show significant separation trends in positive ion mode (Figure 3A) and negative ion mode (Figure 3B). Through MS/MS spectrum comparison, statistical analysis reveals that many lipid characteristics are dysregulated (FC > 2 and t-test p-values < 0.05)

in both the AD group and the control group, particularly in positive ion mode (Figure 3C) and negative ion mode (Figure 3D).

■ **Changes in the Proteomics Network in AD**

Metabolic pathway enrichment analysis revealed several significantly altered pathways include lysine degradation, pyruvate metabolism, glycine, serine, and threonine metabolism, linolenic acid metabolism, and arginine and proline metabolism (Figure 4). Separately, PCA showed a trend of separation between the AD and control groups (Figure 2).

■ **Changes in the Lipidomics Network in AD**

Some dysregulated lipids are upregulated in the AD group, such as Cer 40:9;O3, DG 46:7, TG 45:7, PC O-35:5, DG 25:0, NAE 18:4, NAE 16:1, NAE 16:2, and ST 28:1;O; while some are downregulated, such as DG 44:11, SM 32:7;O3, PC O-33:6, SM 35:7;O3, DG 25:4, DG 26:4, DG 23:4, DG 27:4, DG 24:4, DG 37:7, CAR 18:2, SM 41:1;O2, SM 40:0;O3, SM 40:2;O2, DG O-37:1, and SM 34:2;O3. (Figure 5).

Using the LINEX software, lipidomics networks that connect lipid substances are provided, as shown in Figures 6A, 6B. It showed a global view of lipidome changes

between the control group and the case group. In these networks, each node represents a type of lipid, and each edge between pairs of lipids indicates biochemical reactions that convert one lipid substance into another within or between categories. The color of the edges represents the type of reaction (i.e., FA removal, FA addition, HG removal, HG addition), and the size of the nodes indicates the significance of differences between AD and normal control groups (the larger the node, the more pronounced the change in lipid). In Figure 6A, node colors indicate log-fold changes between the two conditions (red: higher levels in AD patients, blue: lower levels in AD patients), while in Figure 6B, node colors represent lipid categories. Regarding the type of reaction, HG removal is the most common type (highlighted in green in Figure 6B), indicating that pathways involving this type of metabolic reaction are particularly affected by AD. The Figure 6C showed the enrichment network generated by LINEX based on the global network. The algorithm highlights a subnetwork that maximizes

reaction differences between the control and case conditions. The resulting subnetwork consists only of PC and LPC lipid substances and reactions from LPC to PC, which can be catalyzed by phospholipases (such as RHEA: 36231, RHEA: 44068, RHEA: 40579).

Validation of Candidate Biomarkers and Analysis of AD Correlation

Targeted lipid quantification based on LC-MS/MS was performed to quantify 32 lipids. As shown in Figure 7, seven lipids were significantly upregulated in the AD group (Cer 40:9; DG 25:0, DG 46:7, NAE 16:1, PC (20:1/22:5), PC O-35:5, and TG 45:7. Further ROC curve analysis revealed that the AUCs for these seven lipids were greater than 0.8, with Cer 40:9; (AUC 0.884, 95% CI 0.732-0.913), DG 25:0 (AUC 0.824, 95% CI 0.715-0.911), DG 46:7 (AUC 0.884, 95% CI 0.809-0.947), NAE 16:1 (AUC 0.84, 95% CI 0.756-0.916), PC (20:1/22:5) (AUC 0.816, 95% CI 0.715-0.912), PC O-35:5 (AUC 0.877, 95% CI 0.784-0.94), TG 45:7. (AUC 0.835, 95% CI 0.737-0.919).

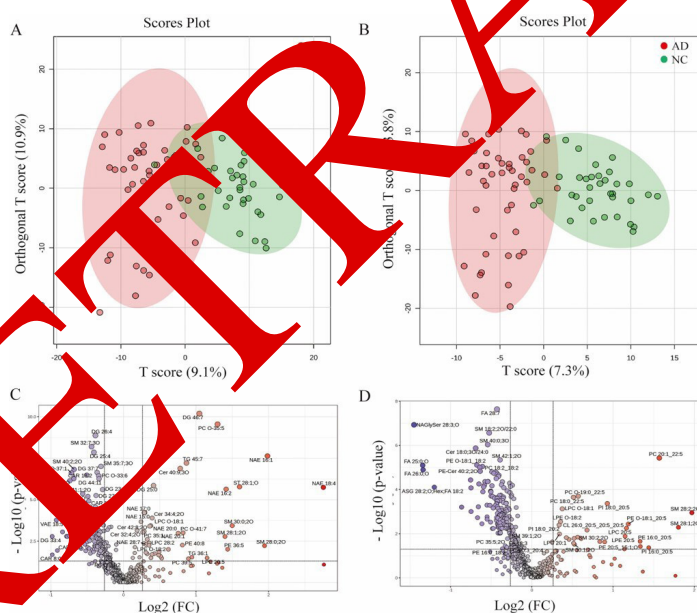


Figure 2. Overview of the untargeted metabolomic results. A) Orthogonal PLS-DA score plot for the metabolites detected in positive ion mode. The samples in different groups are presented by different colors: red, AD (n=47); green, normal control (n=35). Circles represent the 95% confident interval. B) Orthogonal PLS-DA score plot for the metabolites detected in negative ion mode. The samples in different groups are presented by different colors: red, AD (n=47); green, normal control (n=35). Circles represent the 95% confident interval. C) Scatter plots presenting Fold Change (FC) and t-test p-value of the identified metabolites in positive ion mode. The X-axis represents the log₂-transformed FC, and the Y-axis represents the log₁₀-transformed p-value. D) Scatter plots presenting FC and t-test p-value of the identified metabolites in negative ion mode. The X-axis represents the log₂-transformed FC, and the Y-axis represents the log₁₀-transformed p-value.

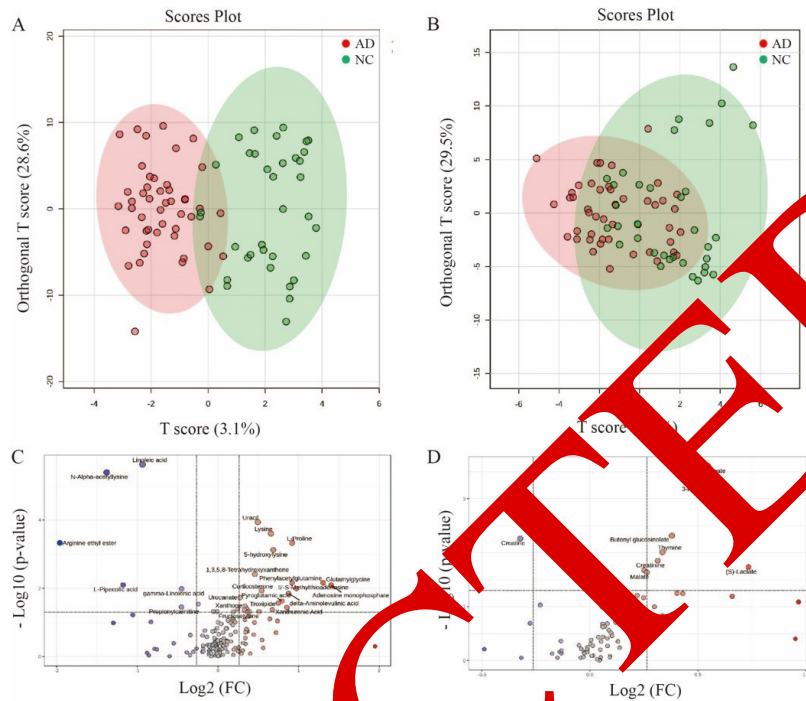


Figure 3. Overview of the untargeted lipidomic results. A) Orthogonal PLS-DA score plot for the metabolites detected in positive ion mode. The samples in different groups are presented by different colors: red, AD (n=47); green, normal control (n=35). Circles represent the 95% confidence interval. B) Orthogonal PLS-DA score plot for the metabolites detected in negative ion mode. The samples in different groups are presented by different colors: red, AD (n=47); green, normal control (n=35). Circles represent the 95% confidence interval. C) Scatter plots presenting Fold Change (FC) and t-test p-value of the identified metabolites in positive ion mode. The X-axis represents the log₂-transformed FC, and the Y-axis represents the log₁₀-transformed p-value. D) Scatter plots presenting FC and t-test p-value of the identified metabolites in negative ion mode. The X-axis represents the log₂-transformed FC, and the Y-axis represents the log₁₀-transformed p-value.

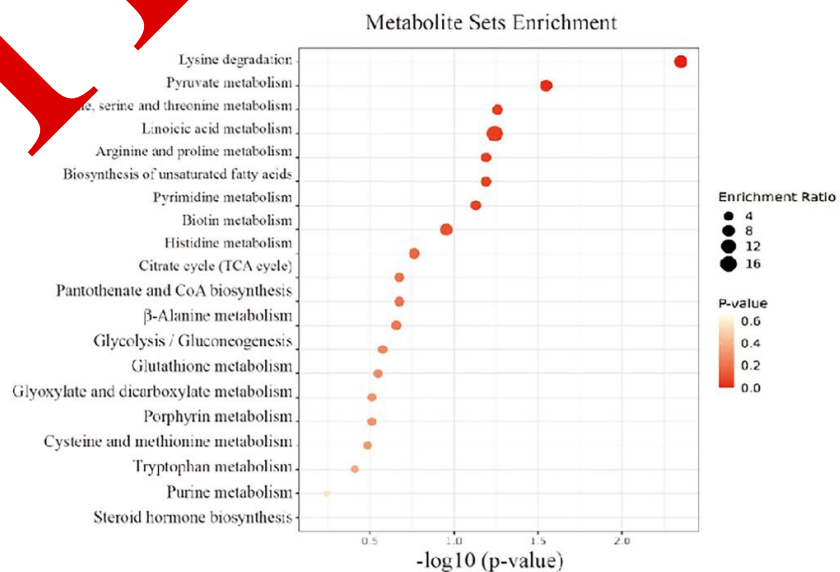


Figure 4. Metabolic pathways enrichment analysis of differential metabolites was conducted based on KEGG database (Bubble chart).

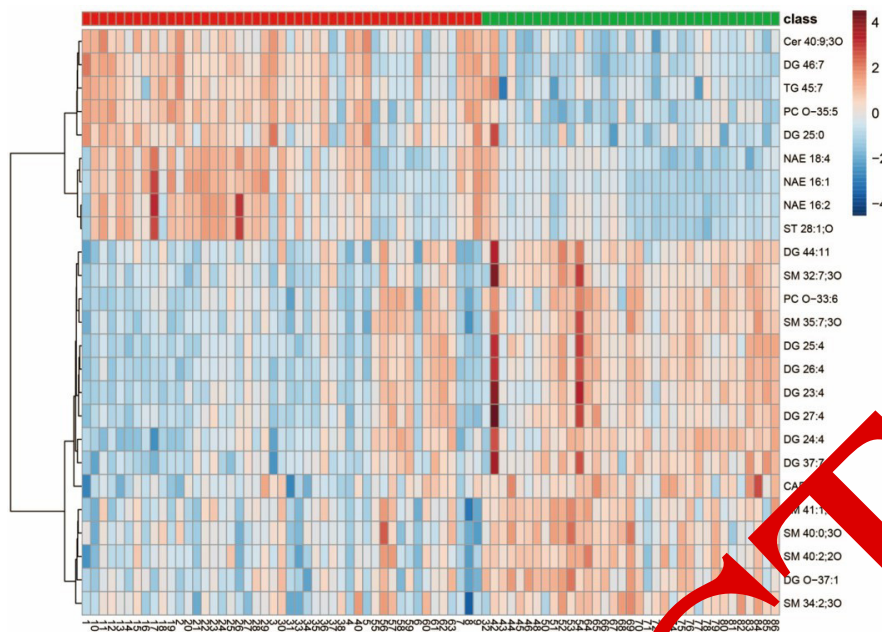


Figure 5. Heat map presenting the expressive patterns of the lipidomic metabolomics in the blood. Sample category is presented in red (AD, n=47 pooled biological replicates) and green (Heath control, HC, n=35 pooled biological replicates), and the intensity of protein is presented from blue (low intensity) to red (high intensity).

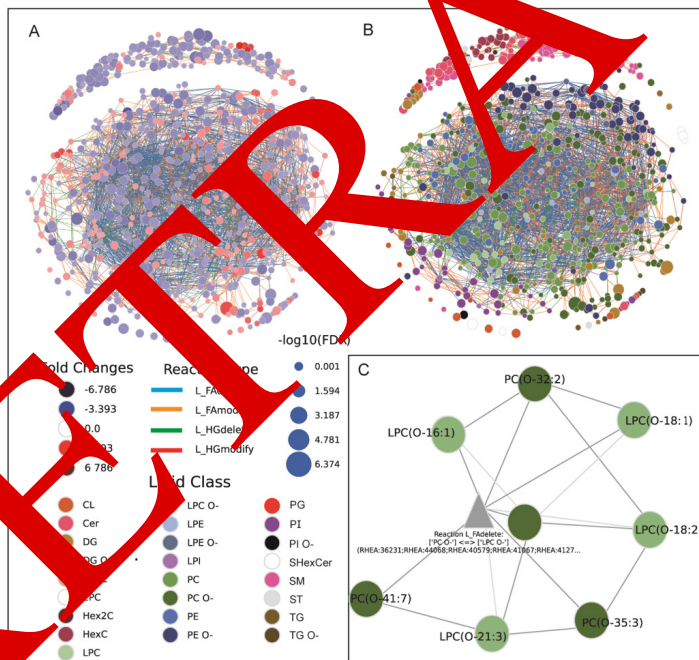


Figure 6. LINEX lipid network based on untargeted lipidomic data. Each node represents a lipid species, and each edge between a pair of nodes indicates a biochemical reaction transforming the lipid species into each other within one class or between classes. Edge colors indicate the reaction types, and node sizes indicate the negative log₁₀ FDR corrected p-values of lipid species between the control and case groups. (A) Node colors represent the log fold change between both groups (red: higher level in the cases and blue: lower level in the cases). (B) Node colors represent the lipid classes. (C) LINEX enrichment network with the PC to LPC reaction at the center. Spherical nodes represent lipids, and the colors refer to LPC (Light green) or PC (dark green) lipid species. Triangular nodes represent the enzyme class.

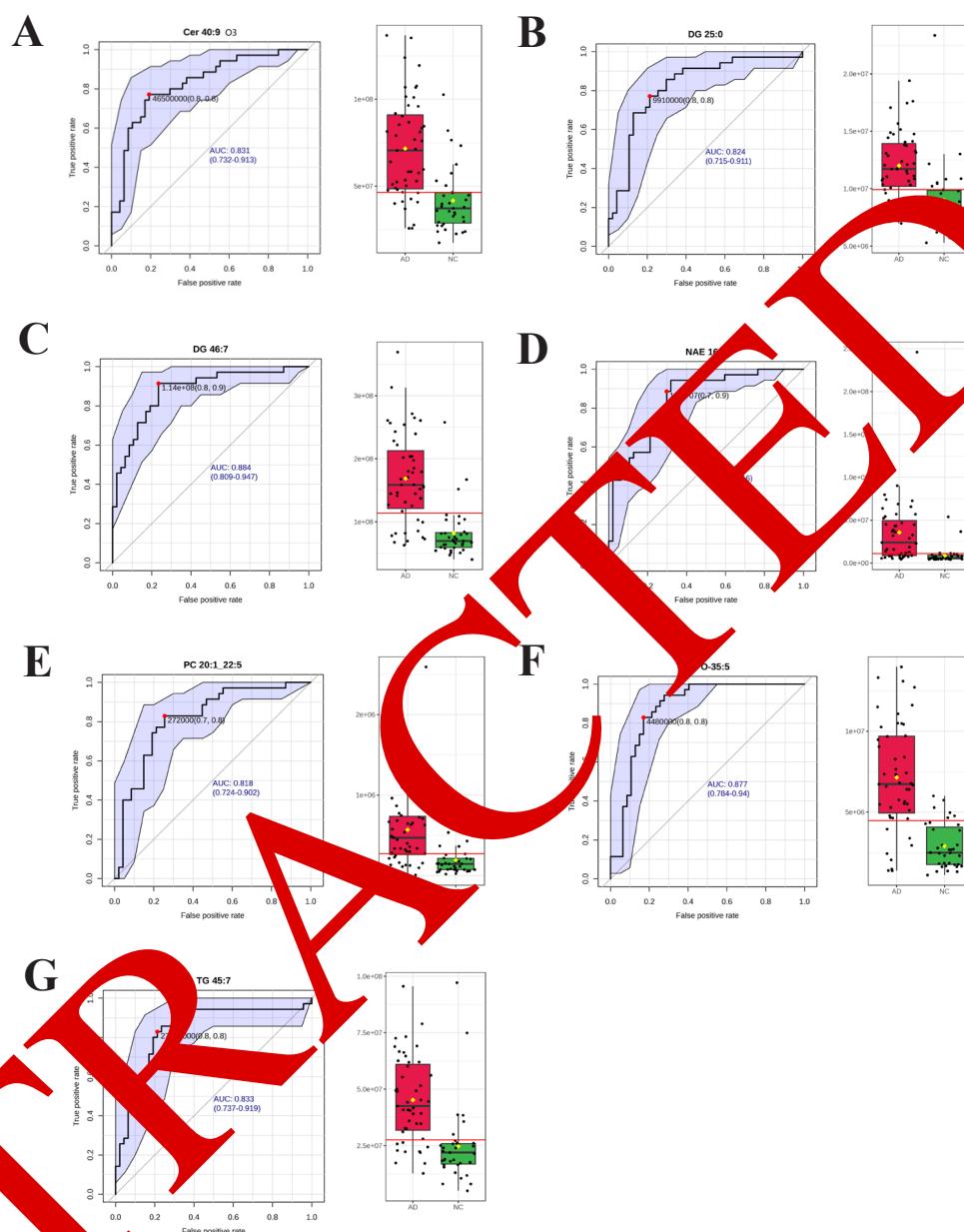


Figure 7 Validation and clinical correlation analysis of the 7 dysregulated lipids. (A-G) ROC curves of lipids (Cer 40:9;O3, DG 25:O, DG 46:7, NAE 16:1, PC 20:1-22:5,PC 0-35:5, PC 0-35:5,TG 45:7 respectively. Red: AD group, n=47; Green: healthy control group, n=35). AUC, 95% confidence intervals, scatter plots, and cutoff values are also shown.

Discussion

In 2024 the Alzheimer’s Association Workgroup revised the diagnostic and staging criteria for AD. The updated framework highlights core 1 biomarkers, including CSF or plasma A β 42, p-tau217, p-tau181, p-tau231, and amyloid PET, all of which map onto either the amyloid beta pathway or the AD tauopathy pathway(Clifford R, et al., 2011).However, CSF testing is invasive and PET imaging is expensive, we want to search for other plasma biomarkers, such as metabolomics markers.

In this study, 82 participants were recruited. The blood samples were quantified by the LC-MS/MS and HPLC plus Q-Exactive HF MS. The analyzed results of Proteomics that lysine degradation, pyruvate metabolism, glycine, serine and threonine metabolism, linolenic acid metabolism and arginine and proline metabolism, were changed in the amino acid metabolic pathways. Further, The results of the lipidomics analysis showed that seven lipids, such as Cer 40:9;O3, DG 25:0, DG 46:7, NAE 16:1, PC(20:1/22:5), PC O-35:5, and TG 45:7,

were markedly increased in the AD group, associated with AUC values greater than 0.8.

Our multi-omics approach has identified a signature of seven plasma lipids that are significantly dysregulated in AD and exhibit promising diagnostic potential. This finding gains mechanistic relevance when considering the specific biological roles of these lipids. For instance, the elevated level of Cer 40:9;O3 aligns with the established link between ceramides and AD pathogenesis. Cer 40:9;O3 (Ceramide) is closely related to AD for potentially linked to $A\beta$. Ceramides are known to directly influence the activity of β - and γ -secretases, the enzymes responsible for generating $A\beta$ from APP. Elevated very-long-chain ceramides (like C40) can promote a lipid raft environment that facilitates the colocalization of these secretases with APP, thereby increasing amyloidogenic processing. Ceramides are potent pro-apoptotic and pro-inflammatory signaling molecules. They can activate astrocytes and microglia (the brain's immune cells), driving the production of pro-inflammatory cytokines like TNF- α and IL-1 β . This chronic neuroinflammation creates a toxic environment that accelerates neuronal damage and synergizes with $A\beta$ pathology [11]. Our observation of elevated plasma ceramide levels in Alzheimer's disease patients further supports its potential value in AD diagnosis. Recent studies have confirmed that long-chain ceramides, such as Cer 40:9;O3, show a significant positive correlation with plasma p-tau217 levels (Rho=0.32-0.753), suggesting that they may amplify tau pathology by activating neuroinflammation (microglia/astrocytes) [13].

Similarly, the increase in TG 41:7 may predict the identification prospects of clinical diagnosis of AD. TG 41:7 (Triacylglycerol) is potentially linked to Energy Metabolism & Oxidative Stress. The high number of double bonds in this triglyceride and its constituent fatty acids, highly susceptible to lipid peroxidation. This peroxidation generates reactive aldehydes like 4-hydroxynonenal (4-HNE), which are profoundly toxic. 4-HNE can adduct to and impair key proteins involved in neuronal energy metabolism (e.g., glucose transporters, mitochondrial enzymes), synaptic function, and $A\beta$ clearance, exacerbating metabolic deficits in the AD brain [14,15].

A decrease in the ether phospholipid PC O-35:5

disrupts cell membrane integrity, increasing the likelihood of contact between β -secretase and APP. A 2025 lipidomics study revealed a negative correlation between PC-type lipids and plasma p-tau181 levels ($r=-0.38$, $p<0.01$), potentially attributable to reduced membrane fluidity rendering tau protein more susceptible to phosphorylation by kinases. Integrating phospholipid profiling with p-tau181 measurement improved the diagnostic AUC for Alzheimer's disease to 0.88 (specificity: 82%), outperforming individual biomarkers [11].

There is no direct mention of a specific association between the lipid PC(20:1/22:5), DG 25:0, DG 46:7, NAE 16:0 and Alzheimer's Disease (AD) in the provided literature. Our research has clarified the relationship between the lipid and AD. There are some potential Mechanisms Linking Phospholipids to Alzheimer's Disease. Phospholipids, including various forms of Phosphatidylcholine (PC), are fundamental building blocks of cell membranes in the brain. The composition of these lipids can influence membrane fluidity, integrity, and the function of proteins embedded within them, such as those involved in generating amyloid-beta peptides.

Changes in specific phospholipids could affect the structure of cell membranes. This might alter the interaction between the Amyloid Precursor Protein (APP) and the secretase enzymes that process it. Depending on the nature of the change, this could potentially facilitate the production of amyloid-beta, a key pathological protein in AD. Phospholipids containing Polyunsaturated Fatty Acids (PUFAs), like the 22:5 fatty acid in PC(20:1/22:5), are particularly susceptible to damage by oxidative stress, which is a known factor in AD progression. Lipids are active signaling molecules. Alterations in phospholipid profiles can drive neuroinflammatory processes, which are a central feature of Alzheimer's disease (AD) pathology. Inflammatory cells in the brain, like microglia, can be activated by damaged lipids or shifts in lipid balance [17]. Widespread lipid metabolism disorder is a recognized core feature in Alzheimer's disease [18]. Abnormal lipid environment may promote the production and aggregation of β -amyloid protein ($A\beta$), as well as exacerbate the excessive phosphorylation of tau protein [19].

When these seven lipids are combined with the p-tau217/ $A\beta$ 42 ratio, they may significantly

reduce the “gray zone” (proportion of indeterminate results). For instance, a dual-cutoff strategy for p-tau217/A β 42 has already decreased the intermediate zone from 16% to 8%, and incorporating the lipid profile could further optimize this [20]. Studies indicate that the combination of p-tau217, A β 42/40, and lipid biomarkers achieves an AUC of 0.957 in preclinical Alzheimer’s disease, approaching the accuracy of PET imaging [21-23], a prospect our findings strongly support.

Limitations

This study has several limitations. First, its single-center, cross-sectional design limits the generalizability of the findings and prevents the assessment of how these lipid biomarkers change throughout the different stages of AD. Future longitudinal, multi-center studies are required to validate our findings and observe the dynamics of these lipid biomarkers. Second, the cognitive assessment relied primarily on the MMSE; incorporating more comprehensive batteries like ADAS-cog and MoCA could provide a deeper understanding. Finally, variations in pre-analytical sample handling and the use of different analytical platforms across laboratories pose challenges for the standardization and widespread adoption of these biomarkers.

Conclusion

In conclusion, our integrated lipidomics and proteomics analysis has identified a panel of seven plasma lipids that are consistently dysregulated in AD and hold significant value as diagnostic biomarkers. These findings not only underscore the role of specific metabolic pathways in AD pathophysiology but also demonstrate the potential of plasma-based lipid profiling as a practical and informative tool for AD diagnosis. Future efforts should focus on the longitudinal validation of these biomarkers in larger, diverse cohorts to fully establish their clinical utility for disease monitoring and early detection.

Acknowledgments

The authors would like to thank all the participants and their guardians for their cooperation and contribution to the development of this protocol. We gratefully acknowledge Prof. Zhiqian Tong (Capital Medical University, Beijing, China) for editing this manuscript and giving suggestions on our study design.

Contributors

Conceptualization: S.Z.Z. and Y.Y.Y.; experiments: T.W.W., X.L.L. and Y.Y.Y.; data analysis and presentation: L.X.L., Z.M. and L.Z.; statistical analysis: T.W.W. and F.M.; writing original draft, review and editing: T.Z., Z.M. and H.Y.W. All authors have read and agreed to the published version of the manuscript.

Patient consent

Informed consent was obtained from all subjects involved in the study. The blood collection process followed strict scientific protocols to ensure compliance with EU-GDPR and relevant data protection regulations. This guaranteed that all personal and health data were treated anonymously, securely and confidentially. No individual information was provided to the research team for subsequent demographic analysis.

Ethics Approval

Ethics approval was obtained from the Medical Ethics Committee of the Beijing Geriatric Hospital (approval number: BJLLYY-2024-009).

Data Availability

The datasets used and/or analysed during the current study available from the corresponding author on reasonable request.

Consent to Participate Declaration

Every human participant provide their consent.

References

1. Karran E, Mercken M, De Strooper B. The amyloid cascade hypothesis for Alzheimer's disease: An appraisal for the development of therapeutics. *Nat Rev Drug Discov* 10(9), 698-712 (2011).
2. Verberk IMW, Slot RE, Verfaillie SCJ, et al. Plasma Amyloid as Prescreener for the Earliest Alzheimer Pathological Changes. *Ann Neurol* 84(5), 648-658 (2018).
3. Food and Drug Administration. FDA clears first blood test used in diagnosing Alzheimer's disease. FDA (2025).
4. Ong SE, Mann M. Mass spectrometry-based proteomics turns quantitative. *Nat Chem Biol* 1(5), 252-262 (2005).
5. Wishart DS. Emerging applications of metabolomics in drug discovery and precision medicine. *Nat Rev Drug Discov* 15(7), 473-484 (2016).
6. Saito K, Matsuda F. Metabolomics for functional genomics, systems biology, and biotechnology. *Annu Rev Plant Biol* 61, 463-489 (2010).
7. Cravatt BF, Simon GM, Yates JR 3rd. The biological impact of mass-spectrometry-based proteomics. *Nature* 450(7172), 991-1000 (2007).
8. Mahajan UV, Varma VR, Griswold ME, et al. Dysregulation of multiple metabolic networks related to brain transmethylation and pyrimine pathways in Alzheimer disease: A targeted metabolomic and transcriptomic study. *PLoS Med* 17(7), e1003012 (2020).
9. Sun L, Jia Y, Shi M, et al. Association between Human Blood Metabolome and the Risk of Alzheimer's Disease. *Ann Neurol* 95(5), 756-767 (2022).
10. Jack CR, Albert MS, Knopman DS, et al. Introduction to the recommendations from the National Institute on Aging-Alzheimer's Association workgroups on diagnostic guidelines for Alzheimer's disease. *Alzheimers Dement* 7(3), 257-262 (2011).
11. Kalkman HO, Smigielski L. Ceramides may Play a Central Role in the Pathogenesis of Alzheimer's Disease: A Review of Evidence and Horizons for Discovery. *Mol Neurobiol* 62(11), 14424-14440 (2025).
12. Doecke JD, Chenna A, Lov M. Combining Lumipulse p-tau181 and Aβ42/40 as confirmatory tests for Aβ positivity prior to disease-modifying therapy. *Alzheimers Dement* 21(9), e70707 (2025).
13. Lehmann S, Gabelle M, Duchiron M. Comparative performance of plasma pTau181/Aβ42, pTau181/Aβ42 ratios, and individual measurements in detecting preclinical amyloidosis. *EBioMedicine* 2025, 105025 (2025).
14. Lee SH, Palle E, Ben Aissa M. Chemoprotective Approach to Characterizing the Role of 4-HNE in Accelerated Cognitive Impairment. *Alzheimers Dement* 12(S7), (2016).
15. Gao Q, Wang L, Sun Y. Oxidative stress: from molecular studies to clinical intervention strategies. *Front Mol Biosci* (2025).
16. Álvarez-Sánchez L, Ferré-González L, Peña-Bautista C. New approach to specific Alzheimer's disease diagnosis based on plasma biomarkers in a cognitive disorder cohort. *Eur J Clin Invest* (2025).
17. Arnsten AFT, Feltri T, K, Barthélemy NT. An integrated view of the relationships between amyloid, tau, and inflammatory pathophysiology in Alzheimer's disease. *Alzheimers Dement* 21(8), e70404 (2025).
18. Fennel H, Mastrob R, Seifried NT. Omics sciences for systems biology in Alzheimer's disease. State-of-the-art of the evidence. *Ageing Res Rev* 69, 101346 (2021).
19. Global, regional, and national burden of Alzheimer's disease and other dementias, 1990-2016: A systematic analysis for the Global Burden of Disease Study 2016. *Lancet Neurol* 18(1), 88-106 (2019).
20. Jack CR Jr, Andrews JS, Beach TG. Revised criteria for diagnosis and staging of Alzheimer's disease: Alzheimer's Association Workgroup. *Alzheimers Dement* 20(8), 1-27 (2024).
21. Livingston G, Sommerlad A, Orgeta V, et al. Dementia prevention, intervention, and care. *Lancet* 390(10113), 2673-2734 (2017).
22. Shi J, Sabbagh MN, Vellas B. Alzheimer's disease beyond amyloid: Strategies for future therapeutic interventions. *BMJ* 371, m3684 (2020).